ORIGINAL PAPER　　　　　　　　　　　　　　　　　　　　　　　　**Open Access**

Transversely isotropic thermoelastic thin circular plate with constant and periodically varying load and heat source

Iqbal Kaur[*] 🄳 and Parveen Lata

Abstract

The present research deals with the deformation in transversely isotropic thermoelastic (TIT) thin circular plate. Rotation effect is studied under thermally insulated as well as isothermal boundaries. The Laplace and Hankel transform techniques have been used to find the solution to the problem. The displacement components, conductive temperature distribution, and stress components with the radial distance are computed in the transformed domain and further calculated in the physical domain using numerical inversion techniques. The effects of rotation and two temperatures are represented graphically. Some specific cases are also figured out from the current research.

Keywords: Transversely isotropic, Thermoelastic, Thin circular plate, Laplace transform, Hankel transform

Introduction

A lot of research has been carried out to predict deformation and heat flow in a continuum using thermoelasticity theories during the past few years. Thick plate, thin plate, and a membrane have a large difference according to their structure. Circular thin plates and membranes are widely used in pressure sensors, microphones, loudspeakers, gas flow metres, optical telescopes, solar powers, radio and radar antennae, and many other devices. Plate theories are beneficial for designs and analyses of these devices. Zhao (2008) described the flexural properties of a plate influenced by its thickness. According to Ventsel and Krauthammer (2001) and Zhao (2008), plates can be classified into three categories: membranes, thin plates, and thick plates depending upon the aspect ratio. The aspect ratio is defined as a/h, where a is the diameter of a plate and h is the thickness of a plate. The plates with aspect ratio $a/h \geq 80...100$ are referred as membranes. It is termed as thin plate with aspect ratio as $8...10 \leq a/h \leq 80....100$. Moreover, if $a/h \leq 8...10$, the plate is termed as thick plate.

Kar and Kanoria (2011) studied the thermoelastic response of fibre-reinforced thin circular disc with three phase lag due to axisymmetric thermoelastic loading. Tripathi, Warbhe, Deshmukh, & Verma, (2017a; Tripathi, Warbhe, Deshmukh, & Verma, 2017b) investigated a quasi-static uncoupled theory of thermoelasticity based on time fractional heat conduction equation for a thin circular plate and studied a thin hollow circular disc with quasi-static uncoupled theory of thermoelasticity with the time fractional derivative of order alpha subjected to a time-dependent heat flux. Bhad and Varghese (2014) studied thermoelastic deformation with annular heat supply on a thin circular plate. Tikhe and Deshmukh (2005; Tikhe & Deshmukh, 2006) considered the inverse problem of transient heat conduction in a thin finite circular plate with integral transform technique and the thin circular plate for unknown heating temperatures in the form of Bessel functions and with integral techniques. Gaikwad (2016; Gaikwad & Deshmukh, 2005; Gaikwad, Ghadle, & Mane, 2012) described the circular plate for known interior temperature under steady-state field, a thin circular plate due to uniform internal energy generation using Hankel transform technique for its solution, and the inverse problem of thermoelasticity in a thin isotropic circular plate. Parveen, Lamba, & Khobragade (2012) examined the thermal deflection of a thin circular plate using boundary conditions of radiation type. Ahire, Hamoud, & Ghadle (2019) studied a problem of thermal stresses in

* Correspondence: bawahanda@gmail.com
Department of Basic and Applied Sciences, Punjabi University, Patiala, Punjab, India

circular plate due to internal moving heat sources with integral transform technique. Also, researchers such as Marin (1998, 1999), Hassan, Marin, Ellahi, & Alamri (2018; Marin, Baleanu, & Vlase, 2017), Marin and Craciun (2017; Marin, Craciun, & Pop, 2016), Marin and Öchsner (2017), Lata and Kaur (Kaur & Lata, 2019; Lata & Kaur, 2019a; Lata & Kaur, 2019c; Lata & Kaur, 2019d), Othman and Marin (2017), and Kumar, Sharma, & Lata (2016a) worked on different theories of thermoelasticity. In spite of all these efforts, no attempt has been made for coupled theory of thermoelasticity of thin circular plate with rotation.

In this paper, we have attempted to study the deformation in transversely isotropic thin circular plate due to isothermal/thermally insulated boundaries. The Laplace and Hankel transform has been used to obtain the general solution of the field equations. The analytical expressions of stresses, conductive temperature, and displacement components are computed in transformed domain. However, the resulting quantities are obtained in the physical domain by using numerical inversion technique. Some particular cases are also discussed.

Basic equations

Following Lata (2017a, 2017b), the constitutive relations and field equations for an anisotropic thermoelastic medium in the absence of body forces and heat sources are:

$$t_{ij} = C_{ijkl}e_{kl} - \beta_{ij}T, \tag{1}$$

$$C_{ijkl}e_{kl,j} - \beta_{ij}T_{,j} = \rho\ddot{u}_i, \tag{2}$$

$$\left(K_{ij}^* + K_{ij}\frac{\partial}{\partial t}\right)\phi_{,ij} = \left(1 + \tau_0\frac{\partial}{\partial t}\right)\left(\beta_{ij}T_0\,\dot{e}_{ij} + \rho C_E\dot{T}\right) \tag{3}$$

where

$$T = \phi - a_{ij}\phi_{,ij}, \tag{4}$$

$$\beta_{ij} = C_{ijkl}\alpha_{ij}, \tag{5}$$

$$e_{ij} = \frac{1}{2}\left(u_{i,j} + u_{j,i}\right). \ i = 1, 2, 3 \tag{6}$$

β_{ij} is the thermal tensor, T is the thermodynamic temperature, τ_0 is the relaxation time, T_0 is the reference temperature, t_{ij} are the components of stress tensor, e_{ij} are the components of strain tensor, u_i are the displacement components, ϕ is the conductive temperature, ρ is the density, C_E is the specific heat, K_{ij} is the thermal conductivity parameter, K_{ij}^* is the materialistic constant, a_{ij} are the two temperature parameters, and α_{ij} is the coefficient of linear thermal expansion. C_{ijkl} are the elastic

parameters with symmetry ($C_{ijkl} = C_{klij} = C_{jikl} = C_{ijlk}$). These symmetries of C_{ijkl} are due to the following:

- The stress tensor is symmetric, which is only possible if ($C_{ijkl} = C_{jikl}$).
- If a strain energy density exists for the material, the elastic stiffness tensor must satisfy $C_{ijkl} = C_{klij}$.
- From stress tensor and elastic stiffness, tensor symmetries infer ($C_{ijkl} = C_{ijlk}$) and $C_{ijkl} = C_{klij} = C_{jikl} = C_{ijlk}$.

And following Kumar, Sharma, & Lata (2016b), the equation of motion for a uniformly rotating medium with an angular velocity $\mathbf{\Omega}$ is:

$$t_{ij,j} = \rho\{\ddot{u}_i + (\mathbf{\Omega} \times \mathbf{\Omega} \times \mathbf{u})\}_i + (2\mathbf{\Omega} \times \dot{\mathbf{u}})_i, \tag{7}$$

where $\mathbf{\Omega} = \Omega\mathbf{n}$, $\mathbf{n}$ is a unit vector representing the direction of axis of rotation, the term $\mathbf{\Omega} \times (\mathbf{\Omega} \times \mathbf{u})$ is the additional centripetal acceleration due to the time-varying motion only, and the term $2\mathbf{\Omega} \times \dot{\mathbf{u}}$ is the Coriolis acceleration.

The components of Lorentz force are:

$$F_i = \mu_0\left(\vec{j} \times \vec{H}_0\right),$$

where $\vec{H}_0$ the is magnetic field intensity vector and $\vec{j}$ is the current density vector.

Method and formulation of the problem

We consider a transversely isotropic thin circular plate of thickness 2b occupying space D defined by $0 \le r \le \infty$, $-h \le z \le h$. Thin plates are usually characterised by the ratio a/h (the ratio between the length of a side, a, and the thickness of the material, h, falling between the values of 8 and 80 as mentioned by Ventsel and Krauthammer (2001). Let the plate be subjected to axisymmetric heat supply thermal shock load applied into its inner boundary having initially undisturbed state at a uniform temperature T_0. We use plane cylindrical coordinates (r, θ, z) with the centre of the plate as the origin (Fig. 1).

As the problem considered is plane axisymmetric, (u, v, w, and ϕ) are independent of θ. We restrict our analysis to two-dimension problem with $\vec{u} = (u, 0, w)$, also applying the transformation:

$$x' = x\cos\phi + y\sin\phi, y' = -x\sin\phi + y\cos\phi, \ z' = z.$$

where ϕ is the angle of rotation in x-y plane, on the set of Eqs. (1)–(3) to derive the equations for TIT solid with two temperatures and with energy dissipation, to obtain:
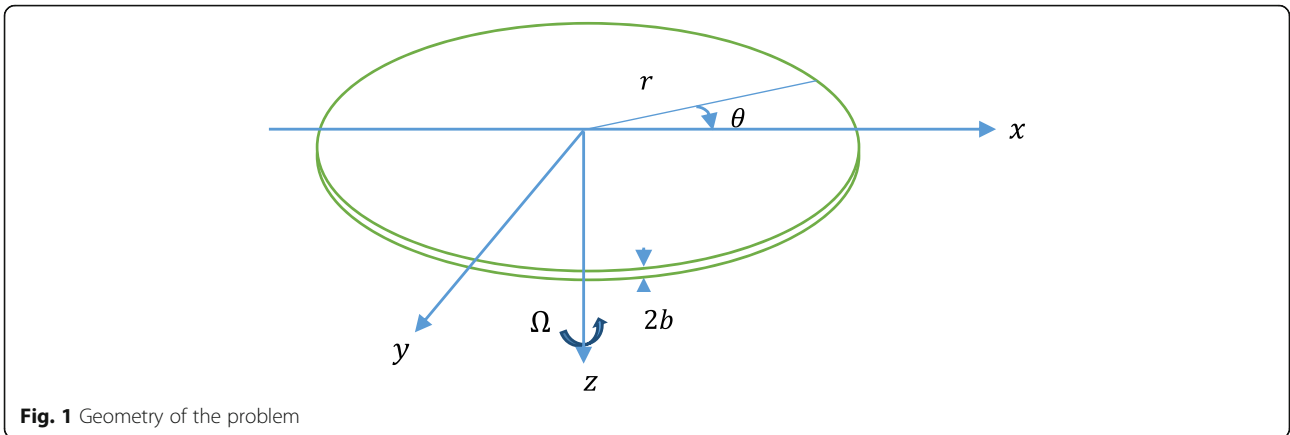
Fig. 1 Geometry of the problem

$$C_{11}\left(\frac{\partial^2 u}{\partial r^2}+\frac{1}{r}\frac{\partial u}{\partial r}-\frac{1}{r^2}u\right)+C_{13}\left(\frac{\partial^2 w}{\partial r\partial z}\right)+C_{44}\frac{\partial^2 u}{\partial z^2}+C_{44}\left(\frac{\partial^2 w}{\partial r\partial z}\right)$$

$$-\beta_1\frac{\partial}{\partial r}\left\{\phi-a_1\left(\frac{\partial^2\phi}{\partial r^2}+\frac{1}{r}\frac{\partial\phi}{\partial r}\right)-a_3\frac{\partial^2\phi}{\partial z^2}\right\}$$

$$=\rho\left(\frac{\partial^2 u}{\partial t^2}-\Omega^2 u+2\Omega\frac{\partial w}{\partial t}\right),$$

$$(8)$$

$$(C_{11}+C_{44})\left(\frac{\partial^2 u}{\partial r\partial z}+\frac{1}{r}\frac{\partial u}{\partial z}\right)+C_{44}\left(\frac{\partial^2 w}{\partial r^2}+\frac{1}{r}\frac{\partial w}{\partial r}\right)$$

$$+C_{33}\frac{\partial^2 w}{\partial z^2}-\beta_3\frac{\partial}{\partial z}\left\{\phi-a_1\left(\frac{\partial^2\phi}{\partial r^2}+\frac{1}{r}\frac{\partial\phi}{\partial r}\right)-a_3\frac{\partial^2\phi}{\partial z^2}\right\}$$

$$=\rho\left(\frac{\partial^2 w}{\partial t^2}-\Omega^2 w-2\Omega\frac{\partial u}{\partial t}\right),$$

$$(9)$$

$$\left(K_1^*+K_1\frac{\partial}{\partial t}\right)\left(\frac{\partial^2\phi}{\partial r^2}+\frac{1}{r}\frac{\partial\phi}{\partial r}\right)+\left(K_3^*+K_3\frac{\partial}{\partial t}\right)\frac{\partial^2\phi}{\partial z^2}$$

$$=T_0\left(1+\tau_0\frac{\partial}{\partial t}\right)\left(\beta_1\frac{\partial\,\dot{u}}{\partial r}+\beta_3\frac{\partial\,\dot{w}}{\partial z}\right)$$

$$+\rho C_E\left(1+\tau_0\frac{\partial}{\partial t}\right)\left\{\dot{\phi}-a_1\left(\frac{\partial^2\,\dot{\phi}}{\partial r^2}+\frac{1}{r}\frac{\partial\,\dot{\phi}}{\partial r}\right)-a_3\frac{\partial^2\,\dot{\phi}}{\partial z^2}\right\}.$$

$$(10)$$

In above equations, we use the contracting subscript notations ($1 \to 11$, $2 \to 22$, $3 \to 33$, $5 \to 23$, $4 \to 13$, $6 \to 12$) to relate C_{ijkl} to C_{mn}. Also a_1 and a_3 are two temperature parameters.

For axisymmetric problem following Lata and Kaur (2019b), the constitutive relations are:

$$t_{rr}=c_{11}e_{rr}+c_{12}e_{\theta\theta}+c_{13}e_{zz}-\beta_1 T,$$

$$t_{zr}=2c_{44}e_{rz},$$

$$t_{zz}=c_{13}e_{rr}+c_{13}e_{\theta\theta}+c_{33}e_{zz}-\beta_3 T,$$

$$t_{\theta\theta}=c_{12}e_{rr}+c_{11}e_{\theta\theta}+c_{13}e_{zz}-\beta_1 T,$$

where

$$e_{rz}=\frac{1}{2}\left(\frac{\partial u}{\partial z}+\frac{\partial w}{\partial r}\right),$$

$$e_{rr}=\frac{\partial u}{\partial r},$$

$$e_{\theta\theta}=\frac{u}{r},$$

$$e_{zz}=\frac{\partial w}{\partial z},$$

$$T=\phi-a_1\left(\frac{\partial^2\phi}{\partial r^2}+\frac{1}{r}\frac{\partial\phi}{\partial r}\right)-a_3\frac{\partial^2\phi}{\partial z^2},$$

$$\beta_{ij}=\beta_i\delta_{ij},\ \ K_{ij}=K_i\delta_{ij,}$$

$$\beta_1=(c_{11}+c_{12})\alpha_1+c_{13}\alpha_3,$$

$$\beta_3=2c_{13}\alpha_1+c_{33}\alpha_3.$$

To facilitate the solution, the following dimensionless quantities are introduced:

$$r'=\frac{r}{L},\ \ z'=\frac{z}{L}, t'=\frac{c_1}{L}t, u'=\frac{\rho c_1^2}{L\beta_1 T_0}u, w'$$

$$=\frac{\rho c_1^2}{L\beta_1 T_0}w, T'=\frac{T}{T_0}, t_{zr}'=\frac{t_{zr}}{\beta_1 T_0}, t_{zz}'=\frac{t_{zz}}{\beta_1 T_0}, \Omega'$$

$$=\frac{L}{C_1}\Omega, \phi'=\frac{\phi}{T_0}, a_1'=\frac{a_1}{L^2}, a_3'=\frac{a_3}{L^2},$$

$$(11)$$

where $c_1^2=\frac{c_{11}}{\rho}$, and L is a constant of dimension of length.

Using the dimensionless quantities defined by Eq. (11) in Eqs. (8)–(10) and after that suppressing the primes and applying the Laplace and Hankel transforms defined by:

$$f^*(r,z,s) = \int_0^\infty f(r,z,t)e^{-st}dt, \tag{12}$$

$$\tilde{f}(\xi,z,s) = \int_0^\infty f^*(r,z,s)rJ_n(r\xi)dr. \tag{13}$$

on the resulting quantities, we obtain:

$$\left(-\xi^2-s^2+\Omega^2+\delta_2 D^2\right)\tilde{u} + [\xi\delta_1 D-2\Omega s]\tilde{w}$$
$$+\left(\xi\left(1-a_3 D^2\right)+a_1\xi^3\right)\tilde{\phi} = 0, \tag{14}$$

$$(\delta_1\xi D+2\Omega s)\tilde{u}+\left(\delta_3 D^2-\delta_2\xi^2-s^2+\Omega^2\right)\tilde{w}$$
$$-\left(\frac{\beta_3}{\beta_1}D\left[\left(1-a_3 D^2\right)+\xi^2 a_1\right]\right)\tilde{\phi} = 0, \tag{15}$$

$$\delta_4\left(s+\tau_0 s^2\right)\xi\tilde{u}-\delta_5\left(s+\tau_0 s^2\right)D\tilde{w}$$
$$+\left(-\delta_6\left(s+\tau_0 s^2\right)\left(1+\xi^2 a_1\right)-\left(K_1^*+\frac{C_1}{L}K_1 s\right)\xi^2\right.$$
$$+D^2\left.\left(K_3^*+\frac{C_1}{L}K_3 s+a_3\delta_6\left(s+\tau_0 s^2\right)\right)\right)\tilde{\phi} = 0, \tag{16}$$

where

$$\delta_1 = \frac{c_{13}+c_{44}}{c_{11}}, \quad \delta_2 = \frac{c_{44}}{c_{11}}, \quad \delta_3 = \frac{c_{33}}{c_{11}}, \quad \delta_4$$
$$= \frac{\beta_1^2 T_0}{\rho}, \quad \delta_5 = \frac{\beta_1\beta_3 T_0}{\rho}, \quad \delta_6 = \rho C_E C_1^2,$$

and

$$D \equiv \frac{d}{dz},$$

$$\widetilde{t_{zz}} = \frac{C_{13}}{C_{11}}\xi\tilde{u}+\delta_3 D\tilde{w}-\frac{\beta_3}{\beta_1}\left(1+a_1\xi^2-a_3 D^2\right)\tilde{\phi}, \tag{17}$$

$$\widetilde{t_{rz}} = \delta_2 D\tilde{u}-\xi\delta_2\tilde{w}, \tag{18}$$

$$\widetilde{t_{rr}} = -\xi\tilde{u}+\frac{C_{12}\xi}{C_{11}}\tilde{u}+\frac{C_{13}}{C_{11}}D\tilde{w}-\left(1+a_1\xi^2-a_3 D^2\right)\tilde{\phi}. \tag{19}$$

We will obtain the non-trivial solution of Eqs. (14)–(16) if the determinant of the coefficient $\tilde{u}$, $\tilde{w}$, and $\tilde{\phi}$ vanishes, which yields to the following characteristic equation:

$$AD^6 + BD^4 + CD^2 + E = 0, \tag{20}$$

where

$$A = \delta_2\delta_3\zeta_{12}-\delta_2\zeta_{10}\zeta_8,$$

$$B = \zeta_1\zeta_{12}\delta_3-\zeta_1\zeta_{10}\zeta_8+\delta_2\delta_3\zeta_{11}+\delta_2\zeta_{12}\zeta_6-\delta_2\zeta_{10}\zeta_7-\zeta_2^2\zeta_{12}$$
$$-\zeta_2\zeta_9\zeta_8+\zeta_5\zeta_{10}\zeta_2-\zeta_5\zeta_9\delta_3,$$

$$C = \delta_3\zeta_1\zeta_{11}+\delta_2\zeta_6\zeta_{11}+\zeta_1\zeta_6\zeta_{12}-\zeta_1\zeta_{10}\zeta_7-\zeta_2^2\zeta_{11}$$
$$+\zeta_2\zeta_7\zeta_9-\zeta_5\zeta_6\zeta_9+\zeta_4\zeta_2\zeta_{10}-\delta_3\zeta_4\zeta_9+\zeta_3^2\zeta_{12},$$

$$E = \zeta_6\zeta_1\zeta_{11}-\zeta_4\zeta_6\zeta_9.$$

$$\zeta_1 = -\xi^2-s^2+\Omega^2,$$

$$\zeta_2 = \delta_1\xi,$$

$$\zeta_3 = 2\Omega s,$$

$$\zeta_4 = \xi\left(1+a_1\xi^2\right),$$

$$\zeta_5 = a_3\xi,$$

$$\zeta_6 = -\delta_2\xi^2-s^2+\Omega^2,$$

$$\zeta_7 = -\frac{\beta_3}{\beta_1}\left(1+a_1\xi^2\right),$$

$$\zeta_8 = \frac{\beta_3}{\beta_1}a_3,$$

$$\zeta_9 = \delta_4\left(s+\tau_0 s^2\right)\xi,$$

$$\zeta_{10} = -\delta_5\left(s+\tau_0 s^2\right),$$

$$\zeta_{11} = -\delta_6\left(s+\tau_0 s^2\right)\left(1+a_1\xi^2\right)-\xi^2\left(K_1^*+\frac{C_1}{L}K_1 s\right),$$

$$\zeta_{12} = \left(K_3^*+\frac{C_1}{L}K_3 s+a_3\delta_6\left(s+\tau_0 s^2\right)\right).$$

The solutions of Eq. (20) can be written in the form by making use of the radiation condition that $\tilde{u}$, $\tilde{w}$, $\tilde{\phi} \to 0$ as $z \to \infty$:

$$\tilde{u} = \sum A_i(\xi,s)\cosh(q_i z), \tag{21}$$

$$\tilde{w} = \sum d_i A_i(\xi,s)\cosh(q_i z), \tag{22}$$

$$\tilde{\phi} = \sum l_i A_i(\xi,s)\cosh(q_i z), \tag{23}$$

where A_i, being arbitrary constants,$\pm q_i$ are the roots of Eq. (20), and

$$d_i = \frac{(\zeta_2\zeta_{12}-\zeta_8\zeta_9)q_i^3+\zeta_3\zeta_{12}q_i^2+(\zeta_2\zeta_{11}-\zeta_7\zeta_9)q_i+\zeta_3\zeta_{11}}{(-\zeta_8\zeta_{10}+\delta_3\zeta_{12})q_i^4+(\delta_3\zeta_{11}+\zeta_6\zeta_{12}-\zeta_7\zeta_{10})q_i^2+\zeta_6\zeta_{11}}, \tag{24}$$

$$l_i = \frac{(-\zeta_9\delta_3+\zeta_1\zeta_{10})q_i^2+\zeta_3\zeta_{10}q_i-\zeta_8\zeta_9}{(-\zeta_8\zeta_{10}+\delta_3\zeta_{12})q_i^4+(\delta_3\zeta_{11}+\zeta_6\zeta_{12}-\zeta_7\zeta_{10})q_i^2+\zeta_6\zeta_{11}}, \tag{25}$$

where $i = 1, 2, 3$.

Also, using Eqs. (21)–(23) in expressions (17)–(19), we obtain stress components as:

$$\widetilde{t_{zz}} = \sum A_i(\xi,s)\eta_i \cosh(q_i z) + \sum \mu_i A_i(\xi,s)\sinh(q_i z),$$
(26)

$$\widetilde{t_{rz}} = \sum A_i(\xi,s)M_i \cosh(q_i z) + \sum N_i A_i(\xi,s)\sinh(q_i z),$$
(27)

$$t_{rr} = \sum A_i(\xi,s)R_i \cosh(q_i z) + \sum S_i A_i(\xi,s)\sinh(q_i z),$$
(28)

where

$$\eta_i = \frac{C_{13}}{C_{11}}\xi - \frac{\beta_3}{\beta_1}l_i\left(1 + a_1\xi^2 - a_3 q_i^2\right),$$

$$R_i = -\xi + \frac{C_{12}\xi}{C_{11}} - \left(1 + a_1\xi^2 - a_3 q_i^2\right),$$

$$S_i = \frac{C_{13}}{C_{11}}d_i q_i,$$

$$\mu_i = \delta_3 d_i q_i,$$

$$M_i = \delta_2 d_i \xi,$$

$$N_i = \delta_2 q_i, i = 1,2,3.$$

Boundary conditions

We consider a cubical thermal source and normal force along with vanishing of tangential stress components at the stress-free surface at z = ± h. Mathematically, these can be written as:

$$h_1\frac{\partial\phi}{\partial z} + h_2\phi = \pm g_o F(r,z),$$
(29)

$$t_{zz}(r,z,t) = f(r,t),$$
(30)

$$t_{rz}(r,z,t) = 0.$$
(31)

Here, $h_2 \to 0$ corresponds to thermally insulated boundaries and $h_1 \to 0$ corresponds to isothermal boundaries. Using the dimensionless quantities defined by Eq. (11) on Eqs. (29)–(31) and taking Hankel and Laplace transform of the resulting equations and then using Eqs. (26) and (27) and Eqs. (21)–(23) yields:

$$\sum A_i l_i(h_1 q_i + h_2)\sinh(q_i h) = \pm g_o \tilde{F}(\xi,h),$$
(32)

$$\sum A_i(\xi,s)\eta_i \cosh(q_i h) + \sum \mu_i A_i(\xi,s)\sinh(q_i h) = \tilde{f}(\xi,s),$$
(33)

$$\sum A_i(\xi,s)M_i \cosh(q_i h) + \sum N_i A_i(\xi,s)\sinh(q_i h), = 0.$$
(34)

Solving Eqs. (21)–(23) with the aid of Eqs. (32)–(34) and hence solving Eqs. (26)–(28), we obtain:

$$\tilde{u} = \frac{\tilde{f}(\xi,s)}{\Delta}\{-\chi_1\vartheta_1 + \chi_2\vartheta_2 - \chi_3\vartheta_3\} + \frac{g_o\tilde{F}(\xi,h)}{\Delta}\{\chi_4\vartheta_1 - \chi_5\vartheta_2 + \chi_6\vartheta_3\},$$
(35)

$$\tilde{w} = \frac{\tilde{f}(\xi,s)}{\Delta}\{-\chi_1 d_1\vartheta_1 + \chi_2 d_2\vartheta_2 - \chi_3 d_3\vartheta_3\} + \frac{g_o\tilde{F}(\xi,h)}{\Delta}\{\chi_4 d_1\vartheta_1 - \chi_5 d_2\vartheta_2 + \chi_6 d_3\vartheta_3\},$$
(36)

$$\phi = \frac{\tilde{f}(\xi,s)}{\Delta}\{-\chi_1 l_1\vartheta_1 + \chi_2 l_2\vartheta_2 - \chi_3 l_3\vartheta_3\} + \frac{g_o\tilde{F}(\xi,h)}{\Delta}\{\chi_4 l_1\vartheta_1 - \chi_5 l_2\vartheta_2 + \chi_6 l_3\vartheta_3\},$$
(37)

$$t_{zz} = \frac{\tilde{f}(\xi,s)}{\Delta}\{-\chi_1 G_4 + \chi_2 G_5 - \chi_3 G_6\} + \frac{g_o\tilde{F}(\xi,h)}{\Delta}\{\chi_4 G_4 - \chi_5 G_5 + \chi_6 G_6\},$$
(38)

$$\widetilde{t_{zr}} = \frac{\tilde{f}(\xi,s)}{\Delta}\{-\chi_1 G_7 + \chi_2 G_8 - \chi_3 G_9\} + \frac{g_o\tilde{F}(\xi,h)}{\Delta}\{\chi_4 G_7 - \chi_5 G_8 + \chi_6 G_9\},$$
(39)

$$t_{rr} = \frac{\tilde{f}(\xi,s)}{\Delta}\{-\chi_1 G_{10} + \chi_2 G_{11} - \chi_3 G_{12}\} + \frac{g_o\tilde{F}(\xi,h)}{\Delta}\{\chi_4 G_{10} - \chi_5 G_{11} + \chi_6 G_{12}\},$$
(40)

where

$$G_i = l_i(h_1 q_i + h_2)\theta_i,$$

$$G_{i+3} = \eta_i\vartheta_i + \mu_i\theta_i,$$

$$G_{i+6} = N_i\theta_i + M_i\vartheta_i,$$

$$G_{i+9} = S_i\theta_i + R_i\vartheta_i, i = 1,2,3.$$

$$\Delta = G_1\chi_4 - G_2\chi_5 + G_3\chi_6,$$

$$\Delta_1 = -\tilde{f}(\xi,s)\chi_1 + g_o\tilde{F}(\xi,h)\chi_4,$$

$\Delta_2 = \tilde{f}(\xi, s)\chi_2 - g_o\tilde{F}(\xi, h)\chi_5,$

$\Delta_3 = -\tilde{f}(\xi, s)\chi_3 + g_o\tilde{F}(\xi, h)\chi_6,$

$\chi_1 = [G_2G_9 - G_8G_3],$

$\chi_2 = [G_1G_9 - G_7G_3],$

$\chi_3 = [G_1G_8 - G_2G_7],$

$\chi_4 = [G_5G_9 - G_8G_6],$

$\chi_5 = [G_4G_9 - G_6G_7],$

$\chi_6 = [G_4G_8 - G_5G_7],$

$\vartheta_i = \cosh(q_ih), \theta_i = \sinh(q_ih), i = 1, 2, 3$

Applications

In this section, we discuss the effect of various heat sources on the transversely isotropic thin circular plate.

Constant load and heat source

For constant load and heat source which decays moving away from the centre of the thin circular plate in the radial direction as well as along the axial directions:

$$f(r, t) = H(t), F(r, z) = \frac{1}{\sqrt{r^2 + z^2}} \tag{41}$$

where $H(t)$ denotes the Heaviside function. Applying the Laplace and Hankel transform, on Eq. (41), gives:

$$\overline{f}(\xi, s) = \frac{1}{s}, \tilde{F}(\xi, z) = \frac{e^{-\xi|z|}}{\xi} \tag{42}$$

Periodically varying load and heat source

For periodically varying load and heat source which decays moving away from the centre of the thin circular plate in the radial direction as well as along the axial directions:

$$f(r, t) = T_0 \begin{cases} \sin\dfrac{\pi t}{\gamma}, 0 \le t \le \gamma, \\ 0, t > \gamma. \end{cases} F(r, z) = \frac{1}{r^2 + z^2} \tag{43}$$

Applying the Laplace and Hankel transform, on Eq. (43), gives:

$$\overline{f}(\xi, s) = \frac{T_0\pi\gamma(1 + e^{-s\gamma})}{(\pi^2 + s^2\gamma^2)}, \tilde{F}(\xi, z) = K_0(\xi z) \tag{44}$$

Inversion of the transforms

To find the solution of the problem in physical domain, we must invert the transforms in Eqs. (34)–(39). These equations are functions of ξ and z and hence are of the form $\tilde{f}(\xi, z, \omega)$. To get the function $f(r, z, \omega)$ in the physical domain, first, we invert the Hankel transform using:

$$f(r, z, \omega) = \int_0^\infty \xi\tilde{f}(\xi, z, \omega)J_n(\xi r)d\xi. \tag{45}$$

The last step is to calculate the integral in Eq. (45). The method for evaluating this integral is described in Press, Teukolshy, Vellerling, & Flannery (1986), which uses Romberg's integration with adaptive step size. This also uses the results from successive refinements of the extended trapezoidal rule followed by extrapolation of the results to the limit when the step size tends to zero.

Particular cases

The cases are as follows:

- If $K_{ij}^* = 0, \tau_0 = 0$, then Eqs. (35)–(40) give results for TIT thin plate for classical coupled thermoelasticity.
- If angular velocity of thin plate is taken zero, i.e. $\Omega = 0$, then Eqs. (35)–(40) give results for TIT thin plate without rotation.
- If $K_{ij} = 0, \tau_0 = 0$, we obtain a TIT thin plate without energy dissipation, i.e. GN II theory from Eqs. (35)–(40).
- If $K_{ij} \ne 0 \ne K_{ij}^*, \tau_0 = 0$, we obtain a TIT thin plate with and without energy dissipation, i.e. GN III theory from Eqs. (35)–(40).
- If we take $c_{11} = c_{22} = c_{33}, c_{12} = c_{13}, c_{44} = c_{66}, \beta_1 = \beta_3 = \beta, K_1 = K_3 = K, K_1^* = K_3^* = K^*$, then we obtain the results for the case of cubic crystal materials from Eqs. (35)–(40).
- If we take $c_{11} = c_{33} = \lambda + 2\mu, c_{12} = c_{13} = \lambda, c_{44} = \mu, \beta_1 = \beta_3 = \beta = (3\lambda + 2\mu)\alpha, K_1 = K_3 = K, K_1^* = K_3^* = K^*$, then we obtain results for isotropic rotating thin plate with and without energy dissipation from Eqs. (35)–(40).

Numerical results and discussion

In order to illustrate our theoretical results in the proceeding section and to show the effect of rotation in different forms of boundary conditions as mentioned in applications in above part, we now present some numerical results. Cobalt material is chosen for the purpose of numerical calculation, which is transversely isotropic. The physical data for cobalt material, which is transversely isotropic, is taken from Dhaliwal and Singh (1980) which is given by:

$c_{11} = 3.07 \times 10^{11} Nm^{-2},$

$c_{12} = 1.650 \times 10^{11} Nm^{-2},$
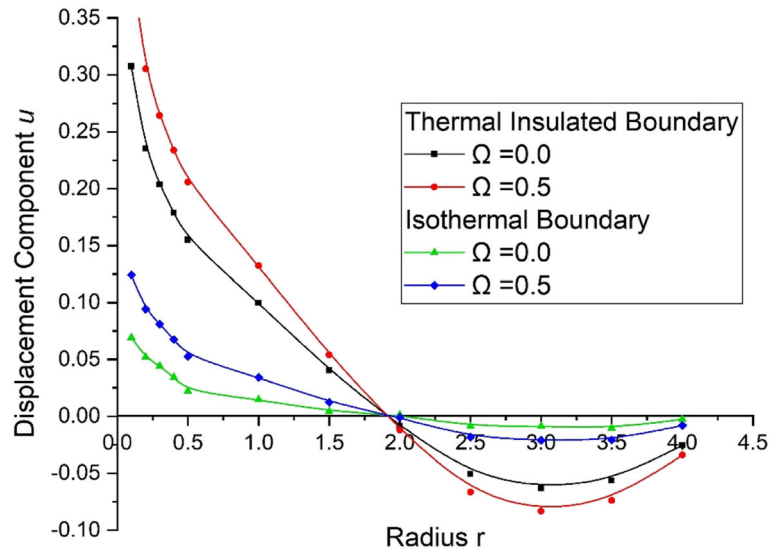
$c_{13} = 1.027 \times 10^{10} Nm^{-2},$

Fig. 2 variations of displacement component *u* with radius *r*

$c_{33} = 3.581 \times 10^{11} Nm^{-2}$

$c_{44} = 1.510 \times 10^{11} Nm^{-2}$,

$C_E = 4.27 \times 10^2 JKg^{-1} \ deg^{-1}$,

$\beta_1 = 7.04 \times 10^6 Nm^{-2} \ deg^{-1}, \rho = 8.836 \times 10^3 Kgm^{-3}$

$\beta_3 = 6.90 \times 10^6 Nm^{-2} \ deg^{-1}$,

$K_1 = 0.690 \times 10^2 Wm^{-1} Kdeg^{-1}, \ K_3$
$= 0.690 \times 10^2 Wm^{-1} K^{-1}$,

$K_1^* = 0.02 \times 10^2 NSec^{-2} \ deg^{-1}$,

$K_3^* = 0.04 \times 10^2 NSec^{-2} \ deg^{-1}$.

$L = 1, \tau_0 = 1, h = 0.01m$

The values of normal force stress t_{zz}, tangential stress t_{zr}, radial stress t_{rr}, and conductive temperature ϕ for a TIT solid with two temperature and thermal relaxation times are illustrated graphically to show the effect of two temperatures.
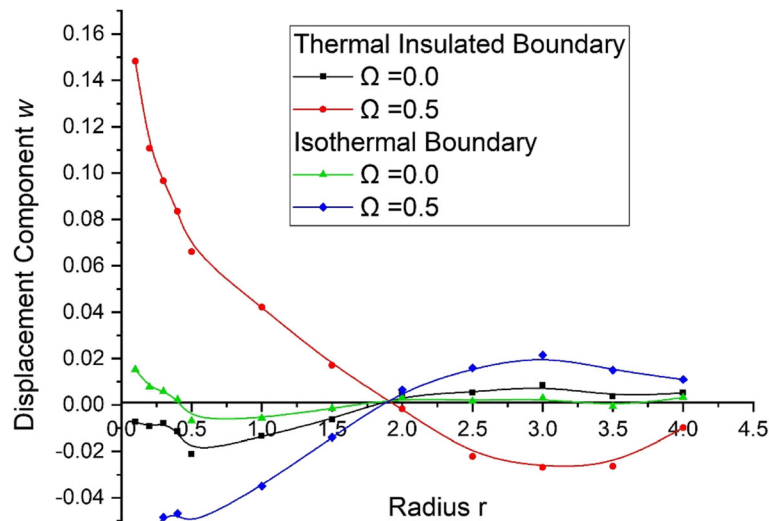

Fig. 3 variations of displacement component *w* with radius r
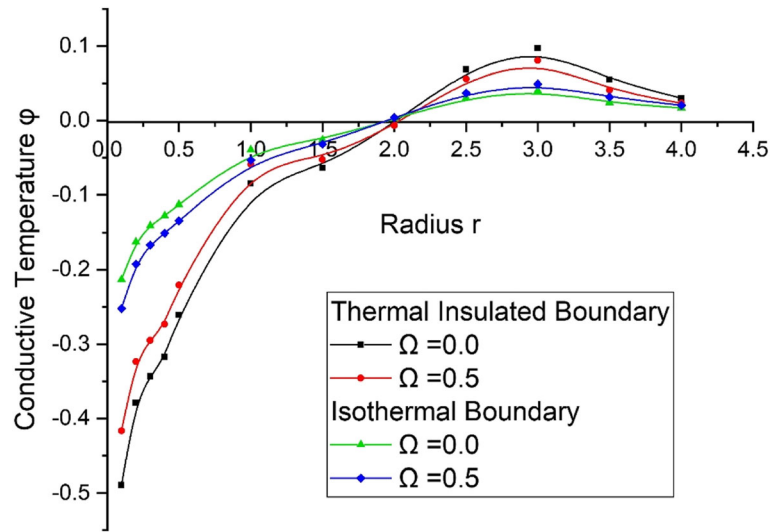
Fig. 4 Variations of conductive temperature φ with radius r

- The solid black line with centre symbol square corresponds to thermal insulated boundaries without rotation.
- The solid red line with centre symbol circle corresponds to thermal insulated boundaries with rotation.
- The solid green line with centre symbol triangle corresponds to isothermal boundaries without rotation.
- The solid blue line with centre symbol diamond corresponds to isothermal boundaries with rotation.

Case 1: Constant load and heat source

Figure 2 shows the variations of displacement component u with radius r for constant load and heat source.

In the initial range of radius r, there is a sharp decrease in the value of displacement component for all the cases. However, for thermal insulated boundary, the displacement component varies more as compared to isothermal boundary conditions. Moreover, away from source applied, it follows oscillatory behaviour. We can see that the rotation has a significant effect on the displacement component in all the cases as there are more variations in u in case of rotation as compared to when rotation is zero.

Figure 3 illustrates the variations of displacement component w with radius r for constant load and heat source. In the initial range of radius r, there is a decrease in the value of displacement component for all the cases. However, for thermal insulated boundary and rotation,
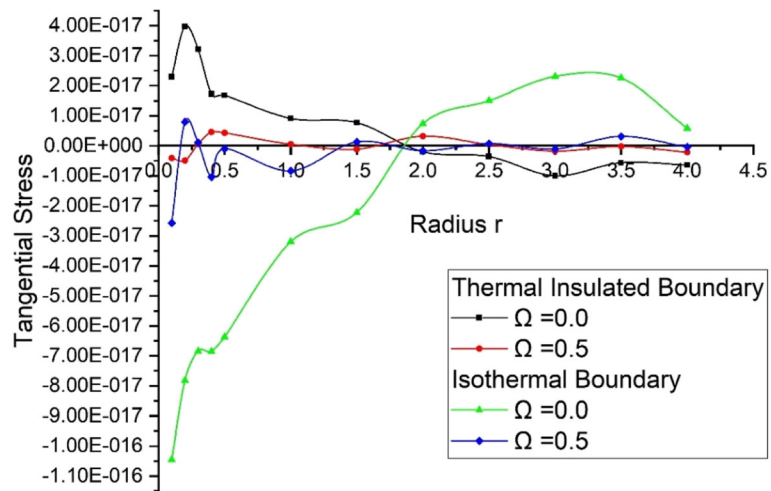

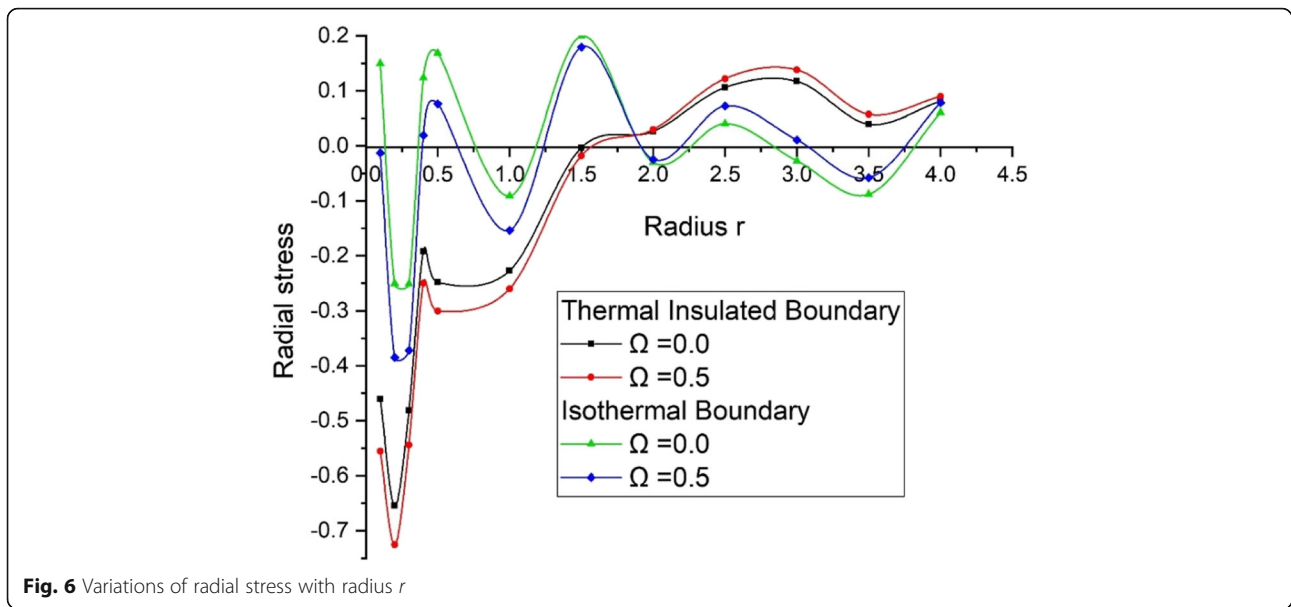**Fig. 5** Variations of tangential stress component t_{zr} with radius r

Fig. 6 Variations of radial stress with radius *r*

the displacement component varies more as compared to isothermal boundaries, with and without rotation. Moreover, away from source applied, it follows opposite oscillatory behaviour. We can see that the rotation has a major effect on the displacement component as there are more variations in *w* in case of rotation, and it behaves opposite for thermal insulated and isothermal boundary conditions.

Figure 4 illustrates the variations of conductive temperature ϕ with radius *r* for constant load and heat source. In the initial range of radius *r*, there is a sharp increase in the value of ϕ for all the cases. However, for thermal insulated boundary and rotation, the conductive

temperature varies more as compared to isothermal boundaries, with and without rotation. Moreover, away from source applied, it follows opposite oscillatory behaviour nearby the zero value.

Figure 5 illustrates the variations of tangential stress component t_{zr} with radius *r* for constant load and heat source. In the initial range of radius *r*, there is a small oscillation in the value of stress component t_{zr} for all the cases. However, for isothermal boundary and without rotation, the stress component t_{zr} varies more as compared to thermal insulated boundaries for both with and without rotation. Moreover, away from source applied, it follows opposite oscillatory behaviour nearby the zero value.
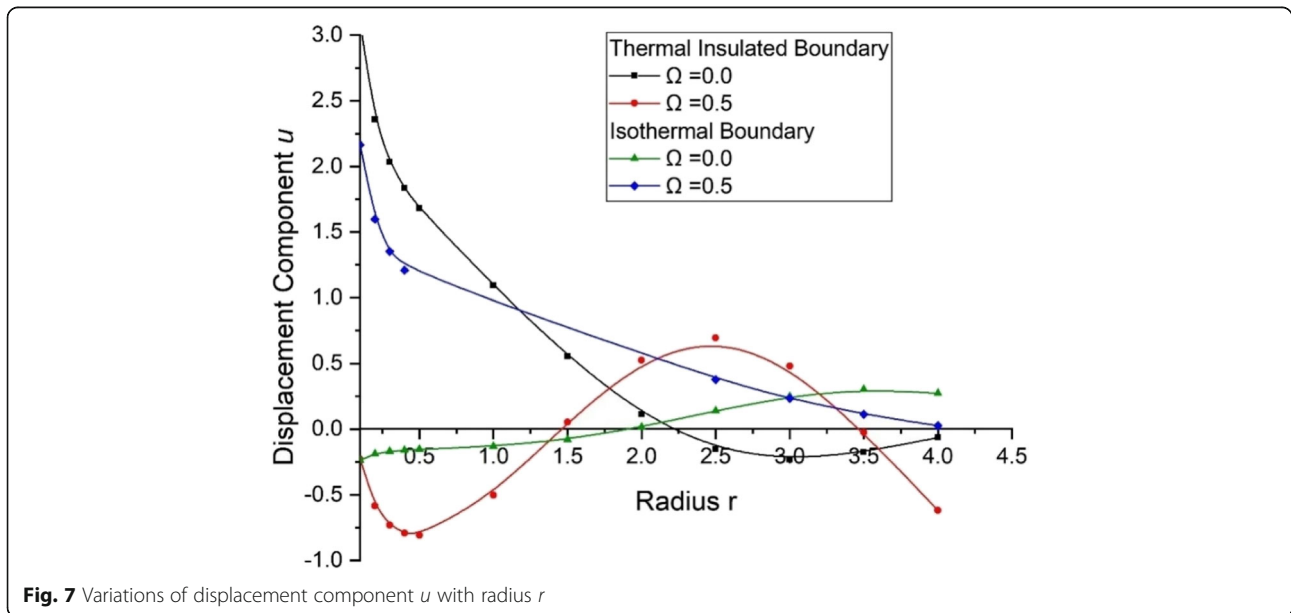

Fig. 7 Variations of displacement component *u* with radius *r*

Fig. 8 Variations of displacement component *w* with radius *r*
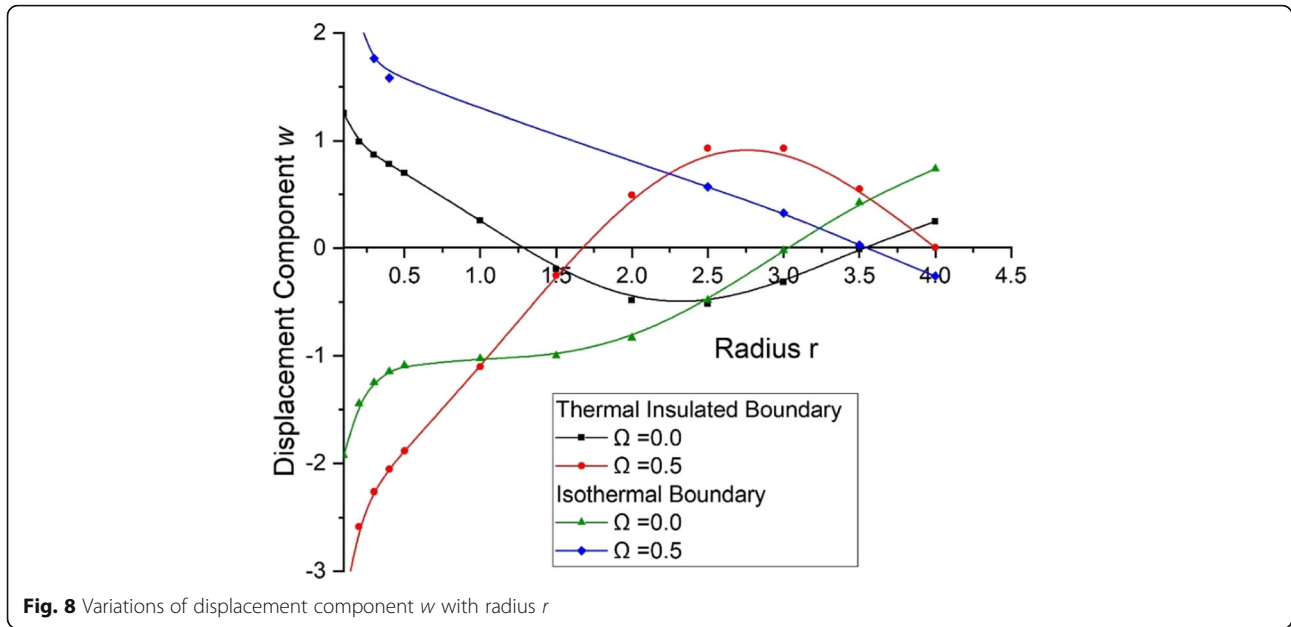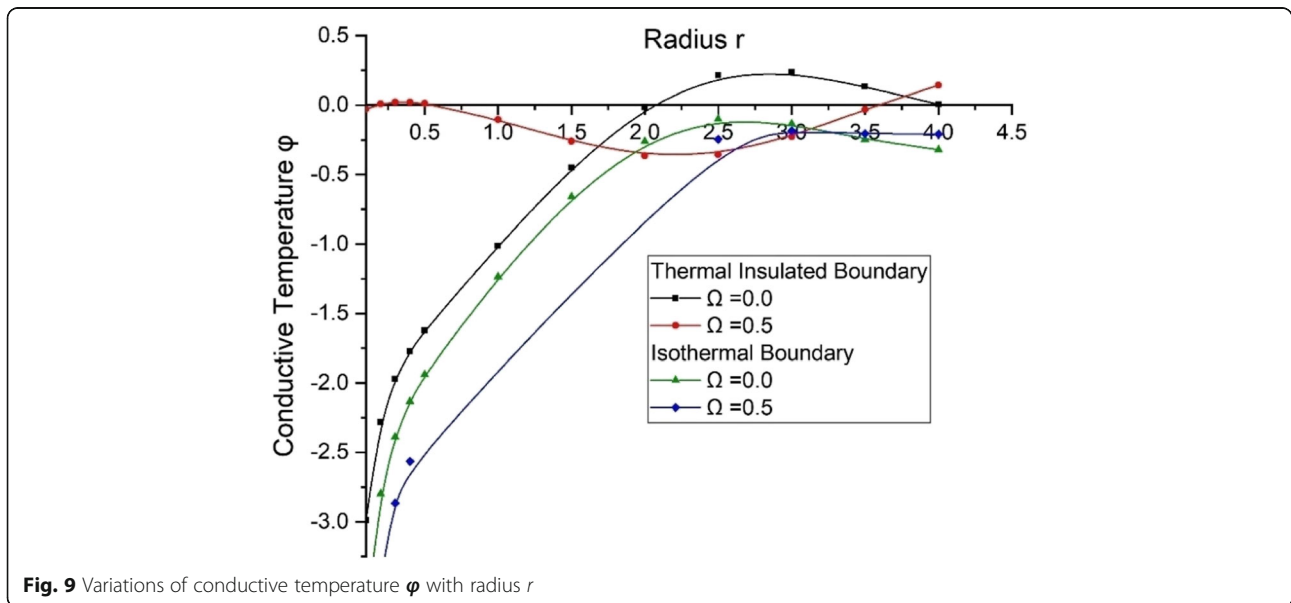
Figure 6 illustrates the variations of radial stress with radius *r*. In the initial range of radius *r* for constant load and heat source, there is a large oscillation in the value of radial stress for all the cases. However, for thermal insulated boundaries, the radial stress varies more as compared to isothermal boundary for both with and without rotation.
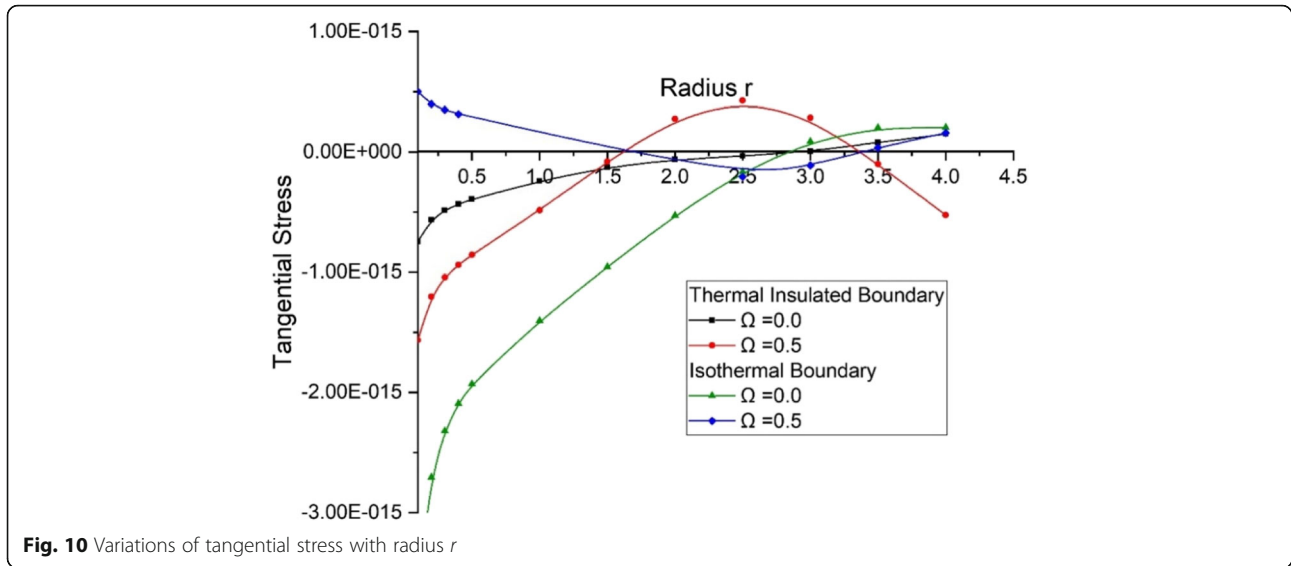
Case II: Periodically varying load and heat source
Figure 7 shows the variations of displacement component *u* with radius *r* due to periodically varying load and heat source. For thermally insulated boundary in the initial range of radius *r*, there is a sharp decrease in the

value of displacement component for all the cases; however, rotation case displacement *w* shows oscillations. However, for thermal insulated boundary, the displacement component varies more as compared to isothermal boundaries conditions. Moreover, away from source applied, it follows oscillatory behaviour. We can see that the rotation has a significant effect on the displacement component as there are more variations in *u* in case of rotation as compared to when rotation is zero.

Figure 8 illustrates the variations of displacement component *w* with radius *r* due to periodically varying load and heat source. In the initial range of distance *x*, there is a decrease in the value of displacement component for

Fig. 9 Variations of conductive temperature *φ* with radius *r*

**Fig. 10** Variations of tangential stress with radius *r*

all the cases. However, for thermal insulated boundary and rotation, the displacement component varies more and is almost opposite as compared to isothermal boundaries, with and without rotation. Moreover, away from source applied, it follows opposite oscillatory behaviour nearby the zero value. We can observed that the rotation as well as isothermal boundary conditions has a significant effect on the displacement component in all the cases as there are more variations in *w* in case of rotation, and it behaves opposite for thermal insulated and isothermal boundary conditions.

Figure 9 illustrates the variations of conductive temperature ϕ with radius *r* due to periodically varying load and heat source. In the initial range of distance *x*,

there is a sharp increase in the value of ϕ for all the cases. However, for thermal insulated boundary and rotation, the conductive temperature varies less and rather oscillates near the plate as compared to isothermal boundaries, with and without rotation. Moreover, away from source applied, it follows opposite oscillatory behaviour near the zero value.

Figure 10 illustrates the variations of tangential stress component t_{zr} with radius *r* due to periodically varying load and heat source. In the initial range of radius *r*, there is a small oscillation in the value of stress component t_{zr} for all the cases. However, for isothermal boundary and without rotation, the stress component t_{zr} varies more as compared to thermal insulated boundaries for

Fig. 11 Variations of radial stress with radius *r*
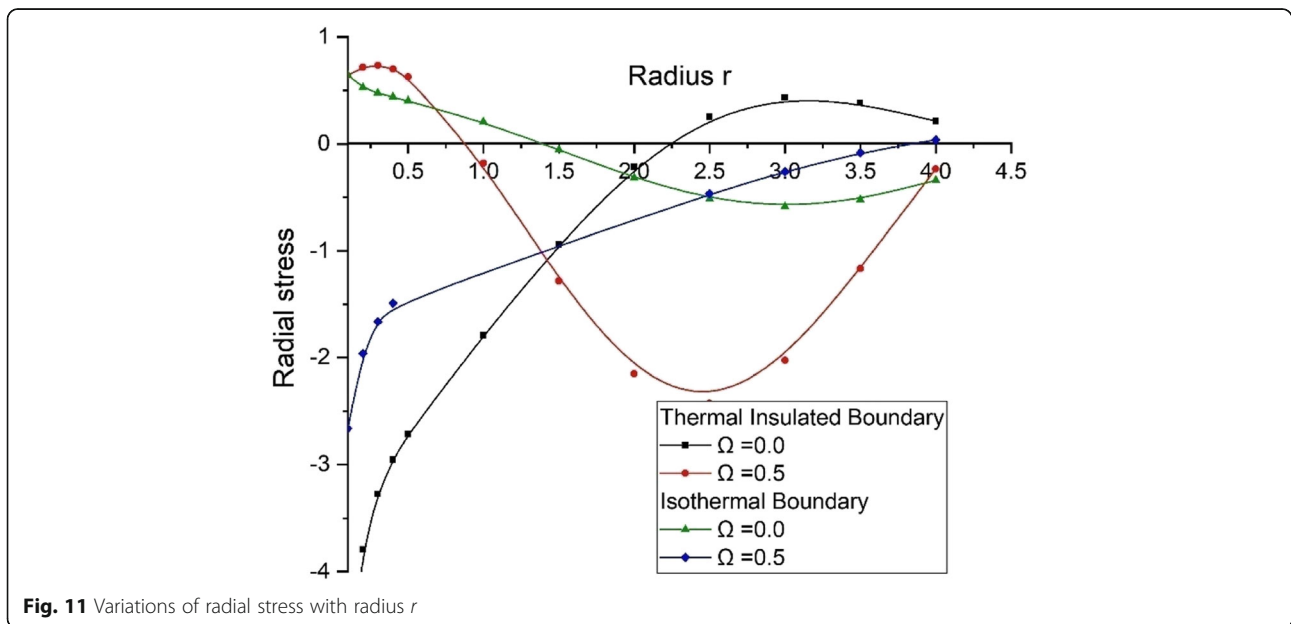
both with and without rotation. Moreover, away from source applied, it follows opposite oscillatory behaviour near the zero value.

Figure 11 illustrates the variations of radial stress t_{rr} with radius r due to periodically varying load and heat source. For thermally insulated boundary and without rotation, the value of radial stress increases for $0 \le r \le 3.0$ and then decreases, while for thermally insulated boundary and with rotation, radial stress t_{rr} first decreases for the range $0 \le r \le 2.5$ and then increases. For isothermal boundary and without rotation, the value oscillates with small amplitude, and for isothermal boundary and with rotation, the value increases but has small increase as opposite of thermally insulated boundary. However, for thermal insulated boundaries, the radial stress varies more as compared to isothermal boundary for both with and without rotation. Moreover, away from source applied, it follows oscillatory behaviour near the zero value.

Conclusion

In this paper, we have discussed the thermoelastic problem for a transversely isotropic thin circular plate with and without rotation and with relaxation time and GN III model. Thermally insulated and isothermal boundary cases for circular edges are considered, and temperature is maintained on upper and lower surface of the circular thin plate. The Laplace and finite Hankel transform technique is used to obtain the numerical results.

In the present research article, conductive temperature, displacement, and stresses along with rotation, two temperatures with thermally insulated and isothermal boundary for constant and periodically varying load have been outlined. Since the thickness of plate is very small, the series solution given here will be definitely convergent. The temperature, displacement, and thermal stresses that are obtained can be applied to the design of pressure sensors, microphones, gas flow metres, optical telescopes, radar antennae, and many other device structures or machines in engineering applications.

Competing interests
The authors declare that they have no competing interests.

References
Ahire, Y. M., Hamoud, A. A., & Ghadle, K. P. (2019). Analysis of thermal stresses in thin circular plate due to moving heat source. *International Journal of Mechanical and Production Engineering Research and Development (IJMPERD), 9*(3), 1285–1292.

Bhad, P. P., & Varghese, D. V. (2014). Thermoelastic analysis on a circular plate subjected to annular heat supply annular heat supply. *Global Journal For Research Analysis, 6*(3), 141–145.

Dhaliwal, R., & Singh, A. (1980). *Dynamic coupled thermoelasticity*. New Delhi: Hindustan Publication Corporation.

Gaikwad, K. R. (2016). Two-dimensional steady-state temperature distribution of a thin circular plate due to uniform internal energy generation. *Applied & Interdisciplinary Mathematics, 3*, 1–10.

Gaikwad, M., & Deshmukh, K. C. (2005). Thermal deflection of an inverse thermoelastic problemin a thin isotropic circular plate. *Applied Mathematical Modelling, 29*, 797–804.

Gaikwad, P. B., Ghadle, K. P., & Mane, J. K. (2012). An inverse thermoelastic problem of circular plate. *The Bulletin of Society for Mathematical Services and Standards, 1*(1), 1–5.

Hassan, M., Marin, M., Ellahi, R., & Alamri, S. (2018). Exploration of convective heat transfer and flow characteristics synthesis by Cu–Ag/water hybrid-nanofluids. *Heat Transfer Research, 49*(18), 1837–1848.

Kar, A., & Kanoria, M. (2011). Analysis of thermoelastic response in a fiber reinforced thin annular disc with three-phase-lag effect. *European Journal Of Pure And Applied Mathematics, 4*(3), 304–321.

Kaur, I., & Lata, P. (2019). Effect of hall current on propagation of plane wave in transversely isotropic thermoelastic medium with two temperature and fractional order heat transfer. *SN Applied Sciences, 1*(900).

Kumar, R., Sharma, N., & Lata, P. (2016a). Effects of thermal and diffusion phase-lags in a plate with axisymmetric heat supply. *Multidiscipline Modeling in Materials and Structures(Emerald), 12*(2), 275–290.

Kumar, R., Sharma, N., & Lata, P. (2016b). Thermomechanical interactions in transversely isotropic magnetothermoelastic medium with vacuum and with and without energy dissipation with combined effects of rotation, vacuum and two temperatures. *Applied Mathematical Modelling, 40*, 6560–6575.

Lata, P. (2017a). Linearly distributed time harmonic mechanical and thermal sources effect at transversely isotropic thermoelastic solids with two temperatures and without energy dissipation. *International Journal of Theoretical and Applied Mechanics, 12*(3), 435–443.

Lata, P. (2017b). A comparison between isotropic and transversely isotropic thermoelastic solids with two temperature and without energy dissipation in frequency domain due to concentrated force. *International Journal of Mechanics and Solids., 9*(1), 77–88.

Lata, P., & Kaur, I. (2019a). Transversely isotropic thick plate with two temperature and GN type-III in frequency domain. *Coupled Systems Mechanics-Techno Press, 8*(1), 55–70.

Lata, P., & Kaur, I. (2019c). Thermomechanical interactions in transversely isotropic thick circular plate with axisymmetric heat supply. *Structural Engineering and Mechanics, 69*(6), 607–614.

Lata, P., & Kaur, I. (2019d). Effect of rotation and inclined load on transversely isotropic magneto thermoelastic solid. *Structural Engineering and Mechanics, 70*(2), 245–255.

Marin, M. (1998). Contributions on uniqueness in thermoelastodynamics on bodies with voids. *Revista Ciencias Matematicas(Havana), 16*(2), 101–109.

Marin, M. (1999). An evolutionary equation in thermoelasticity of dipolar bodies. *Journal of Mathematical Physics, 40*(3), 1391–1399.

Marin, M., Baleanu, D., & Vlase, S. (2017). Effect of microtemperatures for micropolar thermoelastic bodies. *Structural Engineering and Mechanics, 61*(3), 381–387.

Marin, M., & Craciun, E. (2017). Uniqueness results for a boundary value problem in dipolar thermoelasticity to model composite materials. *Composites Part B: Engineering, 126*, 27–37.

Marin, M., Craciun, E., & Pop, N. (2016). Considerations on mixed initial-boundary value problems for micropolar porous bodies. *Dynamic Systems and Applications, 25*(1-2), 175–196.

Marin, M., & Öchsner, A. (2017). The effect of a dipolar structure on the Hölder stability in Green–Naghdi thermoelasticity. *Continuum Mechanics and Thermodynamics, 29*, 1365–1374.

Othman, M., & Marin, M. (2017). Effect of thermal loading due to laser pulse on thermoelastic porous medium under G-N theory. *Results in Physics, 7*, 3863–3872.

Parveen, H., Lamba, N. K., & Khobragade, N. W. (2012). Thermal deflection of a thin circular plate with radiation. *African Journal of Mathematics and Computer Science Research, 5*(4), 66–70.

Press, W. H., Teukolshy, S. A., Vellerling, W. T., & Flannery, B. P. (1986). *Numerical recipes in Fortran. Cambridge*: Cambridge University Press.

Tikhe, A., & Deshmukh, K. (2006). Inverse heat conduction problem in a thin circular plate and its thermal deflection. *Applied Mathematical Modelling, 30*(6), 554–560.

Tikhe, A. K., & Deshmukh, K. C. (2005). Inverse transient thermoelastic deformations in thin circular plates. *Sādhanā Academy Proceeding in Engineering Sciences, 30*(5), 661–671.

Tripathi, J. J., Warbhe, S. D., Deshmukh, K. C., & Verma, J. (2017a). Fractional order thermoelastic deflection in a thin circular plate. *Applications and Applied Mathematics, 12*(2), 898–909.

Tripathi, J. J., Warbhe, S. D., Deshmukh, K. C., & Verma, J. (2017b). Fractional order theory of thermal stresses to a 2 D problem for a thin hollow circular disk. *Global Journal of Pure and Applied Mathematics, 13*(9), 6539–6552.

Ventsel, E., & Krauthammer, T. (2001). *Thin plates and shells: Theory: analysis, and applications*. Taylor & Francis.

Zhao, F. (2008). Nonlinear solutions for circular membranes and thin plates. In *Proceedings of SPIE - The International Society for Optical Engineering*.

Publisher's Note

Springer Nature remains neutral with regard to jurisdictional claims in published maps and institutional affiliations.